Low-Power (1.5 pJ/b) Silicon Integrated 106 Gb/s PAM-4 Optical Transmitter

Joris Lambrecht, Jochem Verbist, Hannes Ramon, Michael Vanhoecke, Johan Bauwelinck, Xin Yin, and Gunther Roelkens

(Top-Scored Paper)

***Abstract*—As next-generation data center optical interconnects aim for 0.8 Tb/s or 1.6 Tb/s, serial rates up to 106 GBd are expected. However doubling the bandwidth of current 53 GBd 4-level pulse-amplitude modulation (PAM-4) transmitters is very challenging, and perhaps unfeasible with compact, non-travelling wave, lumped modulators or lasers. In our previous work, we presented an integrated 4:1 optical serializer with electro-absorption modulators (EAMs) in each path. Transmitter (TX) functionality was shown up to 104 GBd non-return-to-zero (NRZ) On-Off Keying (OOK) or PAM-4. However the performance for PAM-4 was limited by the distortion introduced by the EAM non-linearity. We also presented a real-time, DSP-free 128 Gb/s PAM-4 link with a silicon photonic transmitter using binary driven EAMs in a Mach-Zehnder interferometer (MZI) configuration. By combining two of such half-rate (53 GBd) transmitters in an integrated 2:1-serializer, improved 106 GBd PAM-4 performance is expected without needing to compensate the inherent modulator non-linearity and without requiring faster modulators or drivers. In this paper, we present a Silicon integrated 53 GBd PAM-4 TX as a candidate for integration into 106 GBd PAM-4 2:1 serialized TX. The presented TX consists of two EAMs in an MZI configuration, wirebonded to a low-power 55 nm 4-channel SiGe BiCMOS driver, operating at 1.5 pJ/b (excluding laser). With a reference receiver (RX), transmission at or below the KP4-FEC threshold is shown beyond 1km standard single-mode fiber (SSMF) and up to 2 km non-zero dispersion-shifted fiber (NZ-DSF) at 1565 nm. Furthermore, the integrated TX was combined with an Si-integrated RX consisting of the same EAM component, wirebonded to a 55 nm SiGe BiCMOS transimpedance amplifier (TIA). Both TX and RX were wirebonded on an RF-PCB, with electrical connectivity through transmission lines and 6-inch 50 GHz multi-coax cable connectors. With this electrically connectorized all-EAM TX and RX, PAM-4 link operation is shown up to 40 GBd at 3.9 pJ/b (excluding laser), without using DSP or equalization.**

***Index Terms*—4-Level pulse amplitude modulation (PAM-4), electroabsorption modulator (EAM), photonic integrated circuit (PIC), silicon photonics (SiPh).**

I. Introduction

CURRENT 400 GbE data center interconnects (DCI) follow the 400GBASE standards and proposals for links up to 10 km employing 4, 8 or 16 lanes of respectively 53 GBd PAM-4, 26 GBd PAM-4 or 26 GBd NRZ [7]. As the bandwidth demands of data centers continue to grow, an evolution from 400 Gb/s towards 800 Tb/s and 1.6 Tb/s is envisioned. To avoid an excessive channel count, the lane rates should double. For the fastest links, this implies an increase from the current 106 Gb/s per channel (53 GBd PAM-4) to 212 Gb/s.

A first option could be to double the number of bits per symbol to four, by using PAM-16 at 53 GBd. PAM-16 results in an additional optical power penalty of at least 7 dB and poses extremely stringent requirements on the linearity and response of the digital-to-analog convertors (DACs), analog-to-digital convertors (ADCs) and the analog link components. Furthermore, this involves significant additional digital signal processing (DSP), as is the case for many current PAM-4 interconnects at 53 GBd [8]. A second path could be to consider coherent systems for DCI applications, using 16-QAM (4 bits/symbol) at 53 GBd or higher (e.g. 60 GBd [9]). Coherent links have become the standard in high data-rate long-haul and metro links. The shift to shorter links and inter-data center links is being investigated [10], [11], e.g. by the OIF 400ZR-project [12]. However current state-of-the art coherent modules still have a larger form factor and higher power consumption, e.g. 41.5 mm $\times$ 12.5 mm $\times$ 107.5 mm and 18 W for a 200 Gb/s CFP2-DCO module [13], compared to 19 mm $\times$ 9 mm $\times$ 93 mm and 14 W for a 400 Gb/s QSFP-DD module [14].

A third option is to double the symbol rate to 106 GBd PAM-4. In the traditional single-modulator scheme, this requires the bandwidth of the optical and electrical components to double as well, or to introduce sufficient equalization to compensate a bandwidth deficit accordingly. In this case, the receiver is presented with significant challenges, since input-referred receiver noise tends to increase quickly when increasing bandwidth within the same technology. Additionally, very-low jitter

Manuscript received May 31, 2019; revised July 16, 2019; accepted August 2, 2019. Date of publication August 5, 2019; date of current version January 23, 2020. This work was supported by the EU H2020 projects ICT-Streams (Grant 688172), Teraboard (Grant 688510), and Picture (Grant 780930), and simulation software was provided by VPI. The work of J. Lambrecht and H. Ramon was supported by the Strategic Research Fund (SBO) of the Research Foundation Flanders (FWO). *(Joris Lambrecht and Jochem Verbist contributed equally to this work.) (Corresponding author: Joris Lambrecht.)*

J. Lambrecht, H. Ramon, M. Vanhoecke, J. Bauwelinck, and X. Yin are with the IDLab, Department of Information Technology, Ghent University-IMEC, Ghent 9052, Belgium (e-mail: joris.lambrecht@ugent.be; hannes.ramon@ugent.be; michael.vanhoecke@ugent.be; johan.bauwelinck@ugent.be; xin.yin@ugent.be).

J. Verbist is with the BiFAST, Ghent 9000, Belgium (e-mail: jochem@bifast.io).

G. Roelkens is with the Photonic Research Group, Department of Information Technology, Ghent University-IMEC, Ghent 9052, Belgium (e-mail: gunther.roelkens@ugent.be).

Color versions of one or more of the figures in this paper are available online at http://ieeexplore.ieee.org.

Digital Object Identifier 10.1109/JLT.2019.2933286

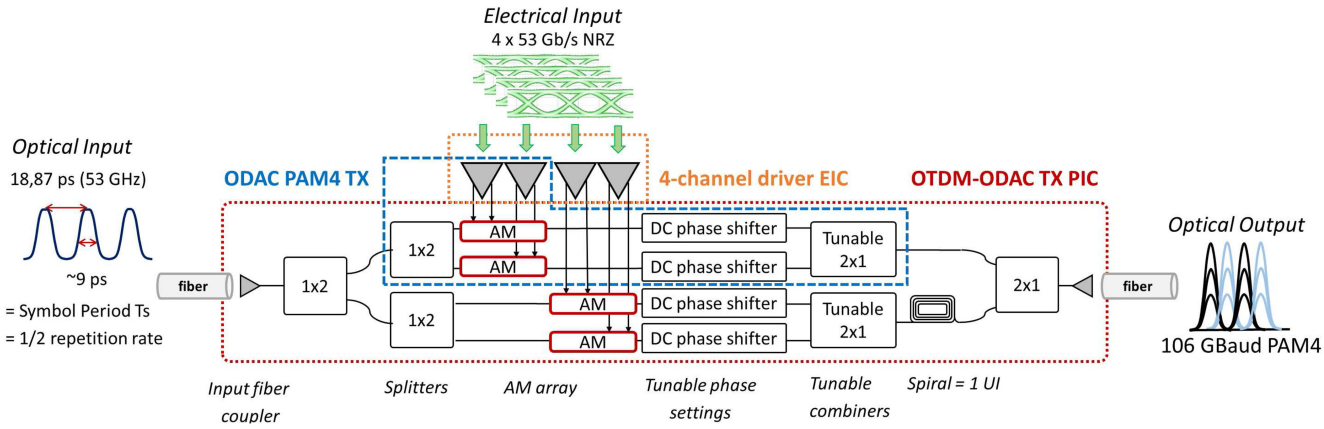

Fig. 1. Proposed Serializer-ODAC transmitter. A single integrated half-rate PAM-4 transmitter, presented in this paper, is highlighted in blue.

clock-and-data recovery (CDR) circuits are required. However at the TX, this option could be advantageous if the strain on the individual components can be limited by properly distributing functionality between photonics and electronics.

In [1], [2], we have demonstrated a 4:1 serializer photonic integrated circuit (PIC) that allowed to generate 104 GBd on-off keying (OOK) and 104 GBd PAM-4 using quarter-rate (26 GBd) electronics. The PAM-4 performance of this PIC was limited by the non-linearity of the intensity modulators (EAMs), thus resulting in distortion, and the inherent optical loss in the 4:1 scheme. Alternatively, as mentioned in [2], we propose a 2:1 optical serializer based on a return-to-zero optical pulse train to avoid 3 dB excess coupler loss over the 4:1 serializer, while leveraging low-power 53 GBd transmitters available today. Furthermore, the generation of the optical pulse train is less involved for 2:1 time domain serialization w.r.t. for 4:1-serialization, since the optical pulse train is effectively a half-rate clock or a half-rate return-to-zero (RZ) optical pulse. To improve the PAM-4 quality, our previously demonstrated optical DAC topology [15] could be a good candidate. This optical DAC does inherently introduce 3 dB optical loss to generate equidistant PAM-4, therefore similar total loss is expected as in [1].

In this paper, we present further work on this half-rate TX. Compared to [3], an integrated PAM-4 TX consisting of a Si PIC with two parallel EAMs, integrated heaters and tunable optical power combiner is wirebonded to a low-power 55 nm SiGe BiCMOS driver chip instead of a combination of probing and external amplifiers. 53 GBd PAM-4 transmission over more than 1 km SSMF and 2 km NZ-DSF is shown while consuming only 160 mW (excluding laser, including on-PIC heaters), or 1.5 pJ/b. The implementation of this integrated half-rate PAM-4 transmitter is an important step towards a 2:1 optically serialized PAM-4 TX with a line rate above 200 Gb/s.

II. Transmitter Architecture

A. Proposed Serializer-ODAC Transmitter

Ideally, combining optical serialization with a 2-bit optical digital-to-analog converter (ODAC) in O-band would allow the use of non-linearly driven intensity modulators (IMs), used as switches, to generate PAM-4. Since PAM-4 is generated optically, the IMs can be driven to their maximal extinction ratio or optical modulation amplitude (OMA) by power-efficient non-linear drivers. In C-band, significant dispersion penalty is expected at these high baudrates, as e.g. the use of dispersion-shifted fiber was necessary for transmission of 104 GBd NRZ and PAM-4 across 1 km SSMF in [2]. The proposed TX is shown in Fig. 1. In contrast to single-modulator solutions, this transmitter concept should enable 106 GBd PAM-4 generation without requiring optical components with significantly higher bandwidths or additional equalization for the TX. The half-rate PAM-4 transmitter is highlighted in blue in Fig. 1.

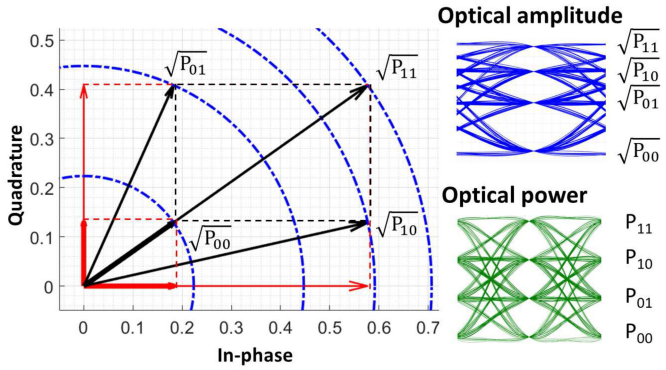

Fig. 2. Operation principle of the parallel-modulator 2-bit optical DAC. The red vectors represent LSB- and MSB-EAM in the on/off state, with limited ER. Equidistant PAM-4 generation results after power detection of the vector sum by a PD.

B. Silicon Integrated PAM-4 Transmitter

The operation principle of the half-rate PAM-4 transmitter is described in [3] and Fig. 2. The input light is split equally in two coherent paths, each with an intensity modulator (IM) with extinction ratio ER and insertion loss IL. The IMs are driven by the least and most significant bit (LSB, MSB) respectively. Afterwards, the two paths are recombined with a tunable phase difference $\Delta\phi$ and a tunable power combining ratio $\alpha : 1-\alpha$. Nominally, assuming IMs with limited ER and non-zero IL, the setting $[\alpha = \frac{1}{3}, \Delta\phi = 90°]$ results in equidistant PAM-4 levels after power detection by a single photodetector (PD) [15]

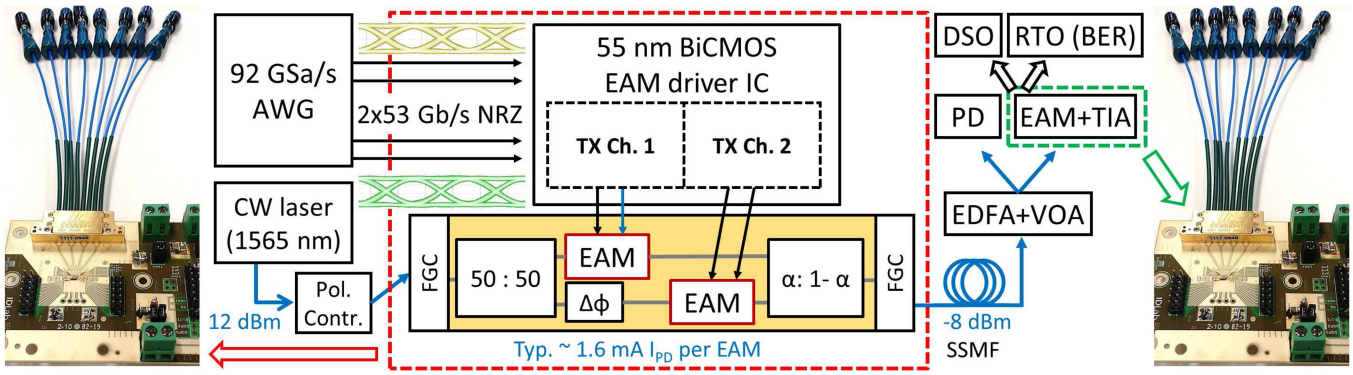

Fig. 3. Experiment setup with connectorized PAM-4 EAM-based TX and RX.

$((i,j) = (MSB, LSB) \in \{0,1\})$:

$$P_{i,j} = \frac{1}{2}\left|\sqrt{\frac{1-\alpha}{IL \cdot ER^{(1-i)}}} + e^{j\Delta\phi}\sqrt{\frac{\alpha}{IL \cdot ER^{(1-j)}}}\right|^2 \quad (1)$$

C. Optical Pulse Generation

Optical serialization relies on a pulsed optical source to enable high baudrates. Mode-locked lasers and comb sources can provide pulses with very small rise and fall times. Significant research effort is being invested in this area, for applications in spectroscopy [16] and communications [17]. Silicon photonics provides a good platform for the heterogeneous integration of arrays of (pulsed) lasers with long optical delays and modulators [18]. Furthermore, the comb spectrum can be so broad that a single pulsed laser can be shared among multiple WDM channels, where each channel is based on optical serialization [2]. Alternatively, optical pulses could be generated by (external) modulation of a continuous-wave (CW) laser, if the optical insertion loss can be kept sufficiently low. For 2:1 serialization, this is analogous to pulse carvers used for return-to-zero (RZ) modulation, as summarized in [19]. Very compact on-chip pulse carvers, e.g. based on parallel microring modulators (MRRs), have also been demonstrated [20].

III. PAM-4 Transmission Experiments

A. Transmitter Experiment Setup

A 92 GSa/s arbitrary waveform generator (AWG) is used to generate two pairs of 300 mVpp binary pseudo-random bit sequence (PRBS) $2^9 - 1$ non-return-to-zero (NRZ) signals at 53 Gb/s. The NRZ signals are decorrelated by introducing a delay difference of at least 20 symbol periods in the AWG. The AWG is connected to the TX assembly, as shown in Fig. 3 (left). The signals are sent through a 6-inch 50 GHz multi-coax connector assembly and RF-transmission lines towards two channels of the EAM driver, which is wirebonded to the printed circuit board (PCB) and to the parallel-EAM PIC (Fig. 4). The PCBs and connector assemblies of both TX and RX were not compensated by the AWG. The non-linear EAM driver amplifies the input signals, reverse biases the EAMs and drives them differentially (Fig. 5) with approximately 2 V_{pp}. The large-signal bandwidth of the driver is approx. 45 GHz [4]. A 1565 nm 12 dBm external laser is coupled into the PIC through fiber-to-grating couplers (FGCs) with approximately 5.5 dB loss per coupler. Eventually, these could be replaced with low-loss edge couplers with a loss of 2 dB [21].

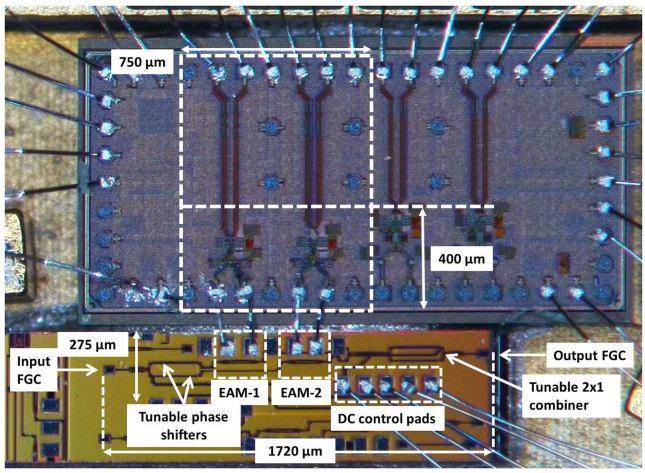

Fig. 4. Si-integrated EAM PAM-4 transmitter. The TX is compact, requiring only 0.275 mm × 1.72 mm on the PIC and 0.4 mm × 0.75 mm on the EIC, including heaters, bondpads and couplers.

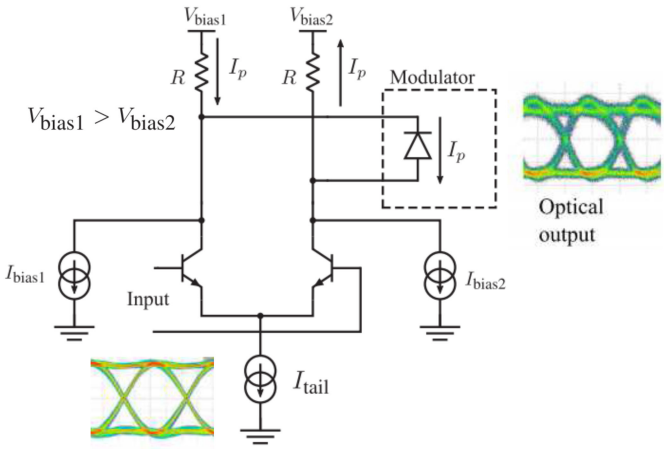

Fig. 5. Schematic of the output stage of the BiCMOS EAM driver [4], which biases and drives the EAM differentially. Nominally, $V_{bias,1} = 3.5$ V and $V_{bias,2} = V_{DD} = 2.5$ V.

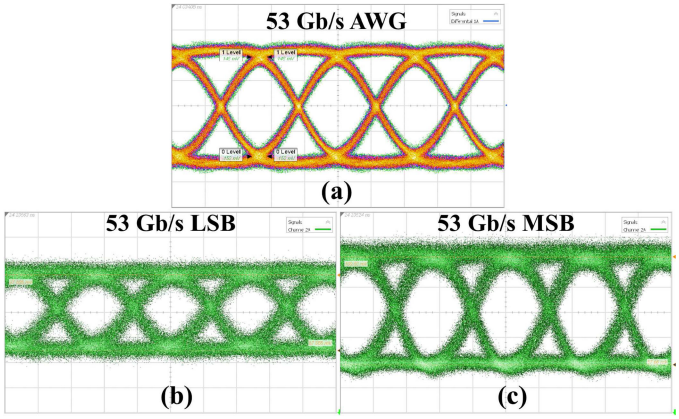

Fig. 6. 53 Gb/s NRZ electrical eye diagram ([a],75 mV/div, 8 ps/div), corresponding optical back-to-back TX eye diagrams of LSB ([b], 10 mV/div, 8 ps/div) and MSB ([c], 12 mV/div, 8 ps/div), measured by disabling MSB or LSB respectively.

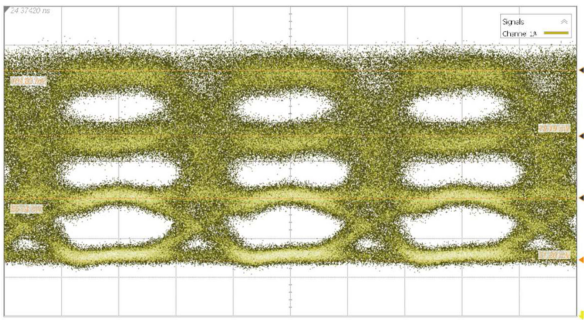

Fig. 7. Back-to-back TX eye diagram at 28 GBd (12 ps/div, 15 mV/div), with an outer extinction ratio $\frac{P_{1,1}}{P_{0,0}}$ of 5.3 dB.

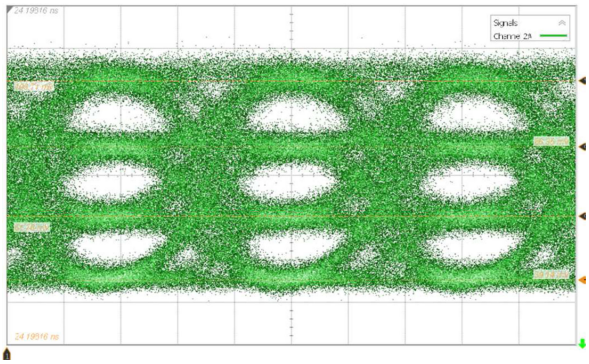

Fig. 8. Back-to-back TX eye diagram at 40 GBd (8 ps/div, 15 mV/div), with an outer extinction ratio $\frac{P_{1,1}}{P_{0,0}}$ of 4.5 dB.

On the PIC, the input light is split equally and routed to both EAMs. Consequently, the EAMs produce the same average photocurrent and present the same effective average load impedance to both driver channels, preserving symmetry. The driver EIC nominally reverse biases the EAMs around -1 V, resulting in approx. 1.6 mA DC photocurrent and 6 dB dynamic insertion loss per EAM. A phase difference is introduced between both paths with a thermal phase shifter. After recombination with thermally-tuned power-combination ratio and the output FGC, the average output power is around -8 dBm. In a previous

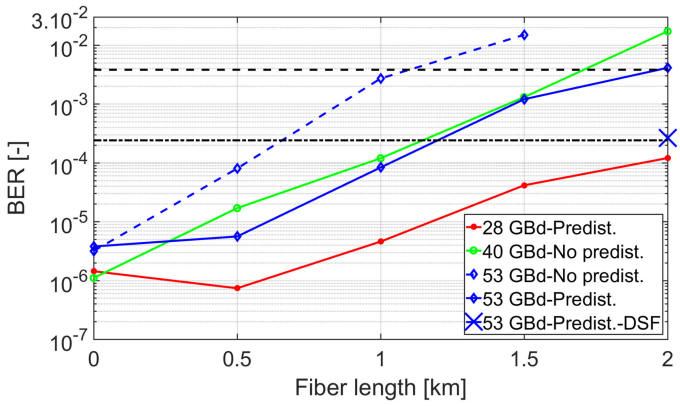

Fig. 9. TX BER vs. fiber length, measured with reference receiver (EDFA + PD) and RTO.

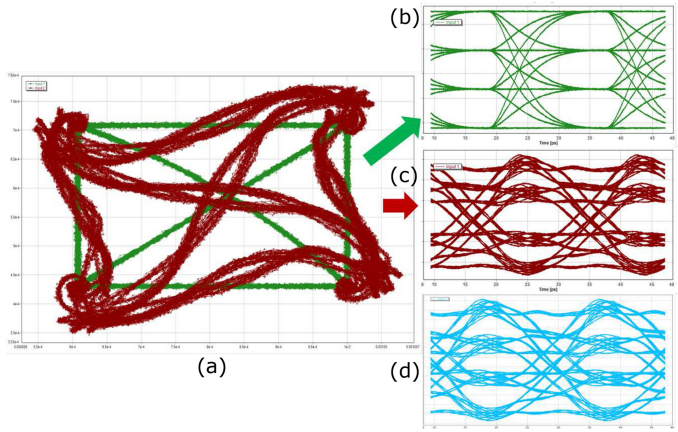

Fig. 10. VPI-simulated 53 GBd TX constellations ([a]) back-to-back vs. ([b]) after 1 km SSMF ([c]), assuming ideal intensity modulators and a $(66:33)$ power combination. With slight predistortion $(60:40)$, [d] is obtained after 1 km SSMF.

implementation of the parallel-EAM TX without integrated drivers [15], the power splitting ratio was fixed. However to obtain equidistant PAM-4, the optical modulation amplitudes (OMAs) of MSB and LSB should satisfy a $2:1$-ratio. Therefore, the EAMs had to be biased and driven differently. As a second-order effect, different EAM bias voltages imply different chirp, altering the behaviour in the presence of fiber dispersion and interfering with the symmetry of the TX. With tunable optical power combining however, a 1.25 dB OMA improvement is expected w.r.t. this electrical equivalent [15] and the inherent symmetry is preserved. As a reference receiver, an erbium-doped fiber amplifier (EDFA) and a DC-coupled 70 GHz highly-linear PD are used. A variable optical attenuator (VOA) ensures constant average optical power (8 dBm) towards the reference PD regardless of the TX settings. Eye diagrams are captured with a digital sampling oscilloscope (DSO), set to 50 GHz bandwidth. For measuring the bit-error ratio (BER), the reference PD is connected directly to a 160 GSa/s 63 GHz real-time oscilloscope. BER is measured on the captured signal after resampling, without any off-line equalization.

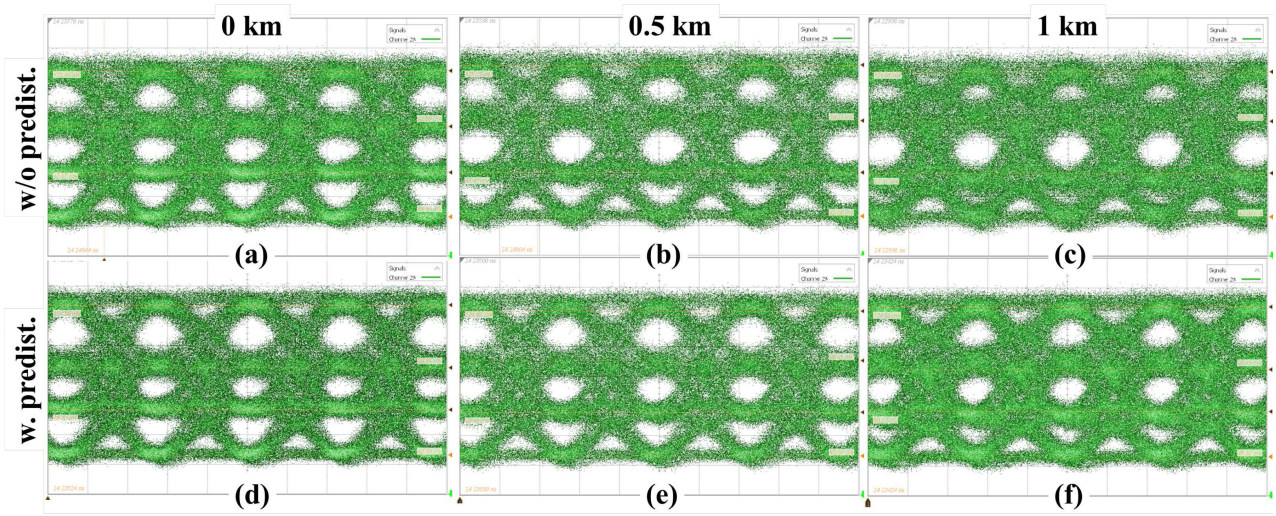

Fig. 11. 53 GBd PAM-4 eye diagrams without predistortion, measured with the EDFA-PD reference receiver, for 0 km (a), 0.5 km (b) and 1 km (c) SSMF; and with predistortion, for 0 km (d), 0.5 km (d) and 1 km (f) SSMF (8 ps/div, 16 mV/div).

B. Transmitter Characterization

Initially, 53 Gb/s TX eye diagrams for the LSB and MSB were measured individually by disabling the AWG output corresponding to the MSB and LSB respectively (Fig. 6). Since the 2:1 MSB-LSB ratio is set optically, both driver channels can be programmed with the same settings.

With both MSB and LSB enabled, after manual fine-tuning of possible MSB-LSB delay mismatch due to slightly different cable pair lengths and PCB transmission line pair lengths, the PAM-4 eye diagrams of Figs. 7 and 8 were obtained at 28 GBd and 40 GBd respectively. The back-to-back 53 GBd TX eye diagram is shown in Fig. 11.a. The TX outer extinction ratio, defined as $\frac{P_{1,1}}{P_{0,0}}$ and measured by the DSO, was 5.3 dB at 28 GBd and 4.5 dB at 40 GBd and 53 GBd.

C. PAM-4 Link Transmission With Reference RX

The BER measured with the reference RX is shown in Fig. 9. At 53 GBd, with the TX optimized for equidistant PAM-4 eyes (Fig. 11.a), a minimal back-to-back BER of $3.17 \cdot 10^{-6}$ was measured (Fig. 9). In this configuration, the BER remains below the KP4 FEC threshold of $2.4 \cdot 10^{-4}$ beyond 500 m standard single mode fiber (SSMF). At 40 GBd, the back-to-back BER is $1.1 \cdot 10^{-6}$ and the BER stays below the KP4-FEC threshold beyond 1 km SSMF. Due to the operating principle of the PAM-4 transmitter and its inherent symmetry, fiber dispersion results in almost symmetrical compression of the outer PAM-4 eyes (Fig. 11).

This is the case even with ideal chirp-less intensity modulators, and is confirmed by VPI simulation (Fig. 10). Due to fiber dispersion, the constellation edges are rotated w.r.t. the original constellation center, which is located in the upper right quadrant of the complex plane. After power detection by a PD, this reduces the eye opening in the outer eyes, while the outer OMA ($P_{1,1} - P_{0,0}$) remains almost identical. Dynamic modulator chirp could further degrade signal quality in the presence of dispersion.

This dispersion-induced compression increases the BER but can be precompensated without sacrificing OMA by thermally tuning the output combiner (and therefore $\alpha : 1 - \alpha$ in Fig. 3), implemented as an MZI with thermal phase shifters. This symmetrically predistorts the TX output, as shown in Fig. 11, improving the 53 GBd BER by approx. one order of magnitude. Equivalently, the sub-KP4-FEC fiber reach is doubled to approx. 1.25 km. With 2 km non-zero dispersion-shifted fiber (NZ-DSF), the BER is just above the KP4-FEC threshold, at $2.62 \cdot 10^{-4}$. The BER penalty in the back-to-back configuration remains small: a BER of $3.77 \cdot 10^{-6}$ is measured with predistortion, vs. $3.17 \cdot 10^{-6}$ without predistortion. Tuning the power combining can keep the 53 GBd BER vs. fiber length below the trace of the 40 GBd BER without predistortion, except for the 40 GBd back-to-back case ($1.1 \cdot 10^{-6}$). For 28 GBd with predistortion, the back-to-back BER ($1.43 \cdot 10^{-6}$) is slightly higher than the BER minimum of $7.35 \cdot 10^{-7}$ at 0.5 km, due to the slightly compressed center eye. The 28 GBd BER remains below the KP4-FEC threshold beyond 2 km SSMF, and below the HD-FEC threshold ($3.8 \cdot 10^{-3}$) beyond 3.5 km SSMF ($1.9 \cdot 10^{-3}$).

D. PAM-4 Si-Integrated Link With EAM-TIA RX

Subsequently the EDFA-PD reference receiver is replaced by an Si-integrated PAM-4 RX, consisting of a 45 GHz 150 mW transimpedance amplifier (TIA), implemented in 55 nm SiGe BiCMOS [5], [6], with the TIA input wirebonded to the same EAM component on an RX-PIC and the output wirebonded to an RF-PCB (Fig. 12). TIA bandwidth and gain are digitally programmable [5]. At 1565 nm and with -2.5 V reverse bias provided by the TIA, the EAM has a responsivity of 0.725 AW^{-1} and 3 dB bandwidth beyond 50 GHz [22].

Electrical connectivity is through an identical 6-inch 50 GHz multi-coax connector assembly. Since only a single high-speed RTO input was available at the time of the measurements, the differential TIA outputs at the multi-coax cable assembly are converted to a single-ended signal by a 67 GHz balun with

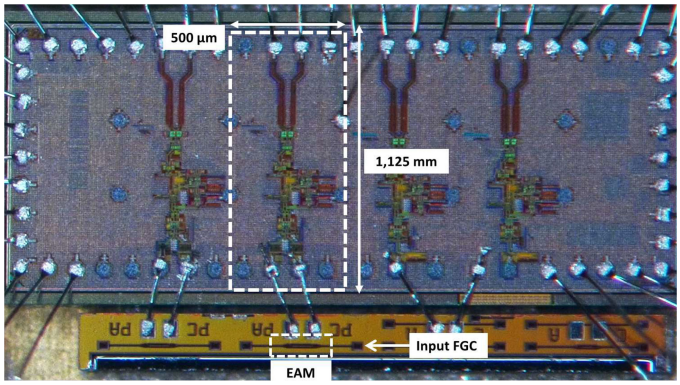

Fig. 12. Silicon integrated EAM PAM-4 receiver. The used TIA channel is highlighted.

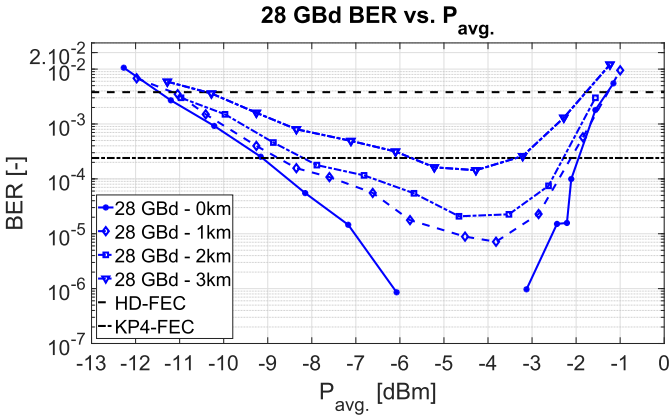

Fig. 13. 28 GBd BER vs. received average optical power.

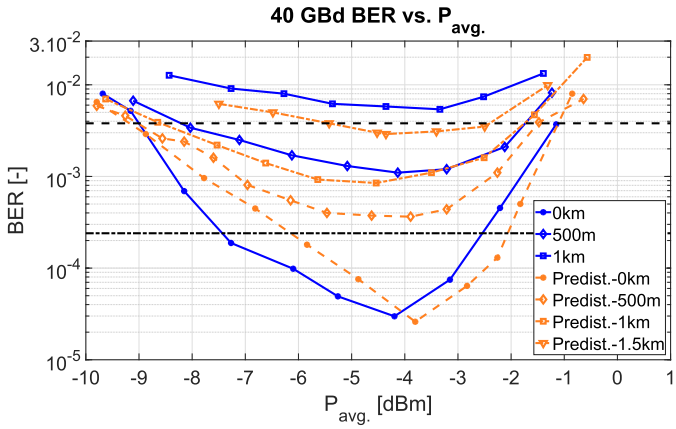

Fig. 14. 40 GBd PAM-4 link BER vs. received average optical power. With slight TX predistortion (tuning $\alpha : 1-\alpha$ in Fig. 3), the 40 GBd link BER is below HD-FEC to 1.5 km SSMF.

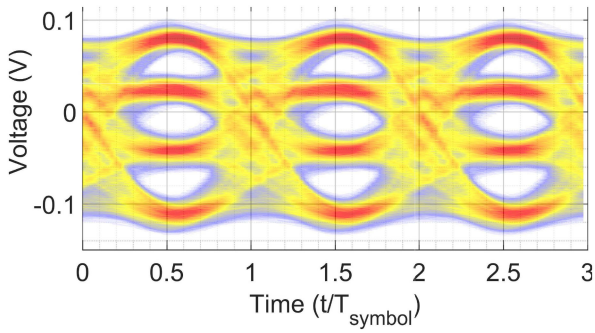

Fig. 15. Back-to-back 28 GBd PAM-4 TIA eye diagram after balun and RTO at −3.2 dBm average optical power (3.6 ps/div, 20 mV/div).

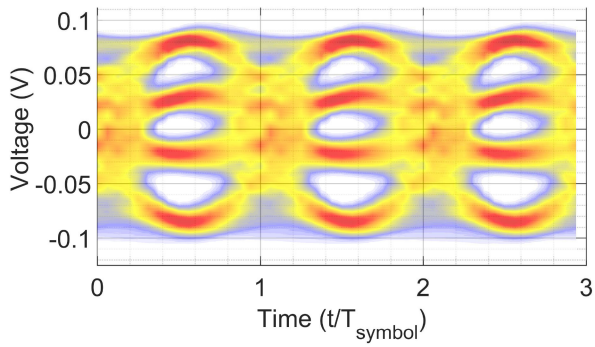

Fig. 16. Back-to-back 40 GBd PAM-4 TIA eye diagram after balun and RTO at −4 dBm average optical power (2.5 ps/div, 20 mV/div).

500 kHz low-frequency cut-off. Although the balun introduces some degradation in the output eye and implies an inherent 6 dB loss, differential signalling improves the signal quality through rejection of common-mode noise sources and even order distortion products. The assembly overhead; i.e. PCB transmission lines, connector assemblies and the balun, was not compensated at neither TX nor RX with DSP or equalization. PAM-4 transmission at 28 GBd and 40 GBd resulted in the BERs of Figs. 13 and 14 respectively. BER is plotted vs. the in-waveguide average optical power at the RX EAM, obtained from the measured photocurrent and responsivity. Figs. 15 and 16 show the 28 GBd and 40 GBd eye diagrams captured at the TIA output. With the connectorized all-EAM TX and RX, PAM-4 transmission below the KP4-FEC threshold is shown up to 3 km SSMF at 28 GBd, while consuming 5.5 pJ/b (excluding laser). At 40 GBd the back-to-back BER is below KP4-FEC and below HD-FEC ($3.8 \cdot 10^{-3}$) up to 1.5 km of SSMF, operating at 3.9 pJ/b (excluding laser). No DSP or symbol equalization was used at the TX nor RX.

IV. Discussion

Table I summarizes the characteristics of state-of-the-art integrated PAM-4 transmitters. Compared to single-modulator solutions [23]–[25], the presented TX differs since it generates PAM-4 from two NRZ-driven EAMs. Therefore no linear drivers are required and the non-linearity of the modulator does not need to be compensated (as in [24]), which can reduce the power consumption of the TX significantly. Compared to classical MZM-transmitters, even with very compact MZMs (only approx. 750 μm length in [25]), the TX is very low-power and compact, occupying only 0.275 mm × 1.72 mm on the PIC and 0.4 mm × 0.75 mm on the EIC. Ref. [26] demonstrates an integrated TX with a very low power consumption and a low Transmitter Dispersion Eye Closure (Quaternary) penalty (TDECQ) of 0.5 dB at 60 °C, however without fiber transmission or BER. Additionally, we have combined the integrated EAM-TX with an integrated EAM-RX, validating link operation up to 40 GBd at 3.9 pJ/b (excluding laser) without using equalization

TABLE I
COMPARISON WITH STATE-OF-THE-ART PAM-4 TRANSMITTERS WITH INTEGRATED DRIVERS

Reference	Data rate [GBd]	Power [pJ/b]	BER [-]	ER [dB]	Modulator	Integration	Driver tech.
[23]	25	30	–	< 13*	Si MZM, segmented	Monolithic	250 nm BiCMOS (EPIC)
[24]	28	18	10^{-6}	5.9	InP EAM (EA-DFB)	External bias-T + cable	0.5 µm InP EIC
[25]	25/28	1.59***/-**	$\approx 2 \cdot 10^{-5}$/-**	5.0/4.7	Si MZM, segmented (optical DAC)	Flip-chip	28 nm CMOS
[26]	53	1.5***	–	2.6	Si MRR	Wirebond	28 nm CMOS
This work	28	3	$7.35 \cdot 10^{-7}$	5.3	Dual SiGe EAMs	Wirebond	55 nm BiCMOS
	53	1.5	$3.17 \cdot 10^{-6}$	4.5			

*Max. 13 dB ER for 28 Gb/s NRZ, while consuming 2 W. **28 GBd BER $>$ KP4-FEC due to RX. ***Excluding heater(s) or temperature control.

or DSP. The same EAM is used as a PD and as a modulator, demonstrating its potential towards a single-device transceiver, simplifying yield optimization for the PIC. Link operation at 53 GBd is under investigation, improvements are expected by avoiding the balun at the RX and by measuring BER in real time.

V. CONCLUSION

We have presented a Silicon integrated, low-power (1.5 pJ/b) 106 Gb/s PAM-4 transmitter by wirebond integration of a parallel-EAM 2-bit optical DAC and a 55 nm SiGe BiCMOS driver IC. It is capable of BERs below or at the KP4-FEC threshold after fiber transmission at 1565 nm over more than 1 km SSMF and 2 km NZ-DSF, without using any equalization or DSP. Compared to state-of-the-art PAM-4 transmitters, the TX is compact and has a very low power consumption by leveraging PAM-4 generation in the optical domain. Therefore, this transmitter is suited for the proposed optically serialized TX, targeting 106 GBd operation at very low power consumption (1.5 pJ/b excluding laser), without requiring drastically faster (linear) modulators or drivers. Furthermore, the same EAM component has been used as a photodetector and wirebonded to a 55 nm SiGe BiCMOS TIA, demonstrating 40 GBd PAM-4 operation with a connectorized TX and RX at 3.9 pJ/b (excluding laser) with only a single active photonic device, without equalization or DSP.

REFERENCES

[1] J. Verbist *et al.*, "104 Gbaud OOK and PAM-4 transmission over 1 km of SMF using a silicon photonics transmitter with quarter-rate electronics," in *Proc. Opt. Fiber Commun. Conf. Exhib.*, Mar. 2019, pp. 1–3.

[2] J. Verbist *et al.*, "4:1 Silicon Photonic Serializer for Data Center Interconnects Demonstrating 104 Gbaud OOK and PAM4 Transmission," *J. Lightw. Technol.*, vol. 37, no. 5, pp. 1498–1503, Mar. 2019.

[3] J. Verbist *et al.*, "Real-time and DSP-free 128 Gb/s PAM-4 link using a binary driven silicon photonic transmitter," *J. Lightw. Technol.*, vol. 37, no. 2, pp. 274–280, Jan. 2019.

[4] H. Ramon *et al.*, "70 Gb/s low-power DC-coupled NRZ differential electro-absorption modulator driver in 55 nm SiGe BiCMOS," *J. Lightw. Technol.*, vol. 37, no. 5, pp. 1504–1514, Mar. 2019.

[5] J. Lambrecht *et al.*, "A 106 Gb/s PAM-4 silicon optical receiver," *IEEE Photon. Technol. Lett.*, vol. 37, no. 7, pp. 505–508, Apr. 2019.

[6] J. Lambrecht *et al.*, "90-Gb/s NRZ optical receiver in silicon using a fully differential transimpedance amplifier," *J. Lightw. Technol.*, vol. 37, no. 9, pp. 1964–1973, Mar. 2019.

[7] "2018 Ethernet Alliance Roadmap," 2018. [Online]. Available: http://www.ethernetalliance.com

[8] "Inphi announces Porrima Gen2 single-lambda PAM4 platform for ...," 2019. [Online]. Available: https://www.globenewswire.com/news-release/2019/02/11/1716536/0/en/Inphi-Announces-Porrima-Gen2-Single-Lambda-PAM4-Platform-for-Hyperscale-Data-Center-and-Cloud-Networks.html

[9] "Toward baseline for 400GBASE-ZR optical specs," 2019. [Online]. Available: http://grouper.ieee.org/groups/802/3/ct/public/adhoc/19_0221/lyubomirsky_3ct_01_190221.pdf

[10] E. Maniloff *et al.*, "400G and Beyond: Coherent evolution to high-capacity inter data center links," in *Proc. Opt. Fiber Commun. Conf. Exhib.*, Mar. 2019, pp. 1–3.

[11] J. Cheng *et al.*, "Comparison of coherent and IMDD transceivers for intra datacenter optical interconnects," in *Proc. Opt. Fiber Commun. Conf. Exhib.*, Mar. 2019, pp. 1–3.

[12] "OIF 400ZR," 2019. [Online]. Available: https://www.oiforum.com/technical-work/hot-topics/400zr-2/

[13] H. Zhang *et al.*, "Real-time transmission of 16 Tb/s over 1020 km using 200 Gb/s CFP2-DCO," *Opt. Express*, vol. 26, no. 6, pp. 6943–6948, Mar. 2018.

[14] "QSFP-DD hardware specification," 2018. [Online]. Available: http://www.qsfp-dd.com/wp-content/uploads/2018/09/QSFP-DD-Hardware-rev4p0-9-12-18-clean

[15] J. Verbist *et al.*, "DAC-less and DSP-free 112 Gb/s PAM-4 transmitter using two parallel electroabsorption modulators," *J. Lightw. Technol.*, vol. 36, no. 5, pp. 1281–1286, Mar. 2018.

[16] N. Picque *et al.*, "Frequency comb spectroscopy," *Nature Photon.*, vol. 13, no. 5, pp. 146–157, Feb. 2019.

[17] H. Hu *et al.*, "Single-source chip-based frequency comb enabling extreme parallel data transmission," *Nature Photon.*, vol. 12, no. e16260, pp. 469–473, Jul. 2018.

[18] Z. Wang *et al.*, "A III-V-on-Si ultra-dense comb laser," *Light, Sci. Appl.*, vol. 6, May 2017, Art. no. e16260.

[19] P. J. Winzer and R. Essiambre, "Advanced modulation formats for high-capacity optical transport networks," *J. Lightw. Technol.*, vol. 24, no. 12, pp. 4711–4728, Dec. 2006.

[20] L. Zhang *et al.*, "Creating RZ data modulation formats using parallel silicon microring modulators for pulse carving in DPSK," in *Proc. Conf. Lasers Electro-Opt./ Conf. Quantum Electron. Laser Sci.*, May 2008, pp. 1–2.

[21] B. Snyder *et al.*, "Packaging and assembly challenges for 50G silicon photonics interposers," in *Proc. Opt. Fiber Commun. Conf. Exhib.*, Mar. 2018, pp. 1–3.

[22] J. Van Campenhout *et al.*, "Silicon photonics for 56G NRZ optical interconnects," in *Proc. Opt. Fiber Commun. Conf. Exhib.*, Mar. 2018, pp. 1–3.

[23] P. Rito *et al.*, "A monolithically integrated segmented linear driver and modulator in EPIC 0.25-μ m SiGe:C BiCMOS platform," *IEEE Trans. Microw. Theory Techn.*, vol. 64, no. 12, pp. 4561–4572, Dec. 2016.

[24] T. Kishi *et al.*, "56-Gb/s optical transmission performance of an InP HBT PAM4 driver compensating for nonlinearity of extinction curve of EAM," *J. Lightw. Technol.*, vol. 35, no. 1, pp. 75–81, Jan. 2017.

[25] S. Tanaka *et al.*, "Ultralow-power (1.59 mW/Gbps), 56-Gbps PAM4 operation of Si photonic transmitter integrating segmented PIN Mach-Zehnder modulator and 28-nm CMOS driver," *J. Lightw. Technol.*, vol. 36, no. 5, pp. 1275–1280, Mar. 2018.

[26] H. Li *et al.*, "A 112 Gb/s PAM4 transmitter with silicon photonics microring modulator and CMOS driver," in *Proc. Opt. Fiber Commun. Conf. Exhib.*, Mar. 2019, pp. 1–3.